

Insulin resistance is a cellular antioxidant defense mechanism

Kyle L. Hoehn^{a,1,2,3}, Adam B. Salmon^{b,1}, Cordula Hohnen-Behrens^a, Nigel Turner^a, Andrew J. Hoy^a, Ghassan J. Maghzal^c, Roland Stocker^c, Holly Van Remmen^b, Edward W. Kraegen^a, Greg J. Cooney^a, Arlan R. Richardson^b, and David E. James^{a,2}

^aDiabetes and Obesity Program, Garvan Institute of Medical Research, 384 Victoria Street, Darlinghurst, NSW 2010, Australia; ^bDepartment of Cellular and Structural Biology, University of Texas Health Science Center at San Antonio, 7703 Floyd Curl Drive, San Antonio, TX 78229-3900; and ^cCentre for Vascular Research, School of Medical Sciences (Pathology) and Bosch Institute, University of Sydney, 94 Parramatta Road, Camperdown, NSW 2036, Australia

Edited by Michael Karin, University of California, San Diego School of Medicine, La Jolla, CA, and approved August 28, 2009 (received for review March 4, 2009)

We know a great deal about the cellular response to starvation via AMPK, but less is known about the reaction to nutrient excess. Insulin resistance may be an appropriate response to nutrient excess, but the cellular sensors that link these parameters remain poorly defined. In the present study we provide evidence that mitochondrial superoxide production is a common feature of many different models of insulin resistance in adipocytes, myotubes, and mice. In particular, insulin resistance was rapidly reversible upon exposure to agents that act as mitochondrial uncouplers, ETC inhibitors, or mitochondrial superoxide dismutase (MnSOD) mimetics. Similar effects were observed with overexpression of mitochondrial MnSOD. Furthermore, acute induction of mitochondrial superoxide production using the complex III antagonist antimycin A caused rapid attenuation of insulin action independently of changes in the canonical PI3K/Akt pathway. These results were validated in vivo in that MnSOD transgenic mice were partially protected against HFD induced insulin resistance and MnSOD+/- mice were glucose intolerant on a standard chow diet. These data place mitochondrial superoxide at the nexus between intracellular metabolism and the control of insulin action potentially defining this as a metabolic sensor of energy excess.

diabetes | mitochondria | superoxide

Insulin resistance (IR) leads to chronic hyperglycemia and/or hyperinsulinemia and these effects contribute to the development of hypertension, type 2 diabetes (T2D), kidney disease, and cardiovascular disease. A major difficulty in the management of metabolic disease concerns the modality of treatment. Some clinical studies, such as the ACCORD trial have strived to normalize blood glucose as a top priority by using a range of therapeutic strategies including insulin injections. Surprisingly, this therapeutic approach was unsuccessful (1). One possibility is that overriding IR may have exacerbated intracellular stress by increasing nutrient delivery to an already stressed cell. Consequently, identifying the mechanistic origin of IR remains a major objective as it may aid therapeutic design.

The origin of IR has been difficult to elucidate in part due to the diverse set of risk factors linked to this condition including overnutrition, physical inactivity, pregnancy, Hepatitis C, polycystic ovarian syndrome, HIV protease inhibitor therapy, and antiinflammatory corticosteroids. Do such factors converge at a common intermediate in the insulin action pathway or does IR represent a collection of distinct cellular disorders? For example, endoplasmic reticulum (ER) stress, proinflammatory responses, oxidative stress, intracellular ceramide accumulation, or the activation of JNK, IKK, or PKC are all currently implicated in the development of IR in overnourished or obese rodents (2, 3). In such models, correcting any one of these intracellular stresses is sufficient to improve IR leading to the possibility that these factors are somehow interconnected. One view is that insulin receptor substrate 1 (IRS1) represents a common convergence point for many defects contributing to IR (4). However, this view has been challenged in that the ability of IRS1-independent receptor tyrosine kinases to activate

metabolism is also impaired in IR (5). This is consistent with previous studies that have failed to observe defects in upstream elements of the insulin signaling pathway under insulin resistant conditions (6).

In the present study, we took a comprehensive approach to identify factor(s) that might unify multiple models of IR. Initially, we compared four diverse models of IR including chronic treatment with insulin, corticosteroids, proinflammatory cytokines, or lipid in both muscle and adipose cell lines. Using minimal exposure to these insults, we have previously observed IR with no consistent change in upstream elements of the insulin signal transduction pathway (5); however, we have now identified a direct correlation between mitochondrial oxidative stress in all models. This is intriguing because reduced mitochondrial function is associated with IR in the elderly and first degree relatives of type 2 diabetics (2). Insults such as inflammation (e.g., tumor necrosis factor- α , TNF) and antiinflammatory corticosteroids (e.g., dexamethasone) cause IR are also associated with reduced mitochondrial function (7, 8), however intriguingly IR insults, such as hyperinsulinemia are shown to enhance mitochondrial oxidative phosphorylation (9) suggesting that mitochondrial oxidative stress may be a more reliable predictor of IR than mitochondrial function. In addition to showing that mitochondrial superoxide ($O_2^{\bullet-}$) is increased in all four models of IR, we also show that either pharmacologic or genetic strategies that override mitochondrial $O_2^{\bullet-}$ reverse or prevent the onset of IR both in vitro and in vivo. Moreover, selective induction of $O_2^{\bullet-}$ using the mitochondrial complex III antagonist antimycin A (AntA) rapidly induced IR and we observed an inverse relationship between the expression of mitochondrial superoxide dismutase (MnSOD) and IR in skeletal muscle of intact mice. We propose that mitochondrial $O_2^{\bullet-}$ is a unifying element of IR principally acting as a nutrient sensor in key metabolic tissues to regulate nutrient intake in accord with energy oversupply.

Results

Mitochondrial Superoxide Stress Precedes IR. We have previously described a reproducible system for studying IR in myotubes and adipocytes in culture relying on the translocation of the facilitative glucose transporter GLUT4 to the plasma membrane (5). This

Author contributions: K.L.H., A.B.S., and D.E.J. designed research; K.L.H., A.B.S., C.H.-B., N.T., A.J.H., and G.J.M. performed research; K.L.H., A.B.S., R.S., H.V.R., E.W.K., G.J.C., and A.R.R. contributed new reagents/analytic tools; K.L.H., A.B.S., and C.H.-B. analyzed data; and K.L.H. and D.E.J. wrote the paper.

The authors declare no conflict of interest.

This article is a PNAS Direct Submission.

¹K.L.H. and A.B.S. contributed equal data

²To whom correspondence may be addressed. E-mail: d.james@garvan.org.au or klh8st@virginia.edu.

³Present address: Department of Pharmacology, University of Virginia, Charlottesville, VA 22908.

This article contains supporting information online at www.pnas.org/cgi/content/full/0902380106/DCSupplemental.

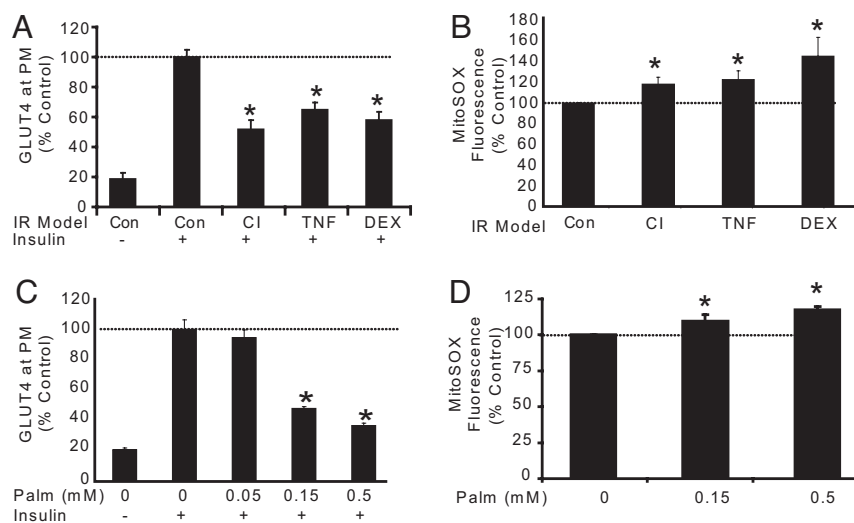


Fig. 1. Multiple models of IR are associated with increased mitochondrial superoxide. (A) 3T3-L1 adipocytes were treated with chronic insulin (CI), TNF- α (TNF), or dexamethasone (DEX) as described in *methods* before acute 100 nM insulin stimulation for 20 min and analysis of GLUT4 abundance at the plasma membrane (PM). The maximal insulin response of control cells was set to 100%. (B) One micromolar MitoSOX Red was added to adipocytes during the final 30 min of IR treatment described in (A). Fluorescence units were measured and normalized as percentage of control treatment. (C) L6 myotubes were incubated with a dose-response of palmitate or BSA/ethanol carrier control for 18 h. Insulin sensitivity was assessed by HA-GLUT4 externalization assay. (D) L6 myotubes were incubated with 5 μ M MitoSOX Red during the final 60 min of treatment. (A–D) Results are displayed as means \pm SEM, $n = 3–4$, *, $P < 0.05$.

process represents one of the earliest defects in IR (2) and so provides a robust measure of this defect. Insulin acutely increased surface levels of GLUT4 by approximately 4-fold in adipocytes and myotubes and this was impaired by approximately 50% in response to hyperinsulinemia (chronic insulin, 10 nM for 24 h; CI), inflammation (2 ng/mL TNF α for 72 h; TNF), steroids (1 μ M dexamethasone for 24 h; DEX), and hyperlipidemia (palmitate, 0.15 mM for 18 h; PALM) defining four separate models of IR (Fig. 1A and C).

Oxidative stress has been implicated in IR, but the precise source of these reactive species is not known. Since mitochondria are also implicated in IR and are a rich source of oxidative end products, we set out to test the hypothesis that mitochondrial oxidative stress may link these two processes as a major cause of IR. Mitochondrial oxidative species are primarily formed by the escape of high energy electrons from complex I and/or complex III of the electron transport chain (ETC). These electrons reduce molecular oxygen creating O₂^{•-}. Therefore, we examined the level of mitochondrial O₂^{•-} in each of our IR models using the mitochondria-targeted O₂^{•-}-sensitive fluorophore MitoSOX Red. MitoSOX Red is hydroethidine (HE) coupled to a mitochondrial targeting lipophilic cation triphenylphosphine (TPP) (10). With one unpaired electron, the O₂^{•-} radical selectively oxidizes the nonfluorescent HE moiety to form the fluorescent product 2-hydroxyethidium (2-OH-E). This increase in fluorescence was used as an index of relative mitochondrial O₂^{•-} production. Increased mitochondrial O₂^{•-} production was observed in each of our models of IR (Fig. 1B and D) signifying an association between IR and mitochondrial O₂^{•-}.

Reversal of IR with Mitochondrial Antioxidants. To determine if mitochondrial O₂^{•-} is upstream of IR we used a pharmacologic approach to decrease mitochondrial O₂^{•-} focusing on palmitate-induced IR in L6 muscle cells. After induction of IR with 12 h of PALM treatment (Fig. 2A) we added drugs aimed at decreasing mitochondrial O₂^{•-} for an additional 6 h (Fig. 2B). Since the ETC is a major site of O₂^{•-} production we first sought to determine if this was the source linked to IR. We used the mitochondrial uncoupler carbonyl cyanide *p*-trifluoromethoxyphenylhydrazone (FCCP) and the respiratory chain complex I inhibitor rotenone. FCCP allows protons to leak back into the mitochondria independent of ATP synthase increasing the speed and efficiency of electron flow and oxygen consumption (11). This results in a more oxidized state of the ETC with less O₂^{•-} production (12–14). Rotenone also reduces O₂^{•-} production and electron flow by partially inhibiting complex I (13, 15). FCCP and rotenone reversed PALM-induced IR in these cells (Fig. 2C) concomitant with

reduced mitochondrial reactive oxygen species (ROS) production (Fig. 2D).

Next we tested the effects of a series of O₂^{•-} scavengers on IR. The mitochondria-targeted superoxide dismutase (SOD) mimetic MitoTEMPO (2-(2,2,6,6-tetramethyl-piperidin-1-oxyl-4-ylamino)-2-oxoethyl)-TPP) reversed IR in a dose dependent manner whereas the TPP moiety or TEMPOL had no effect (Fig. 2E). Two other mitochondria-penetrating SOD mimetics, manganese 5,10,15,20-tetrakis (4-benzoic acid) porphyrin (MnTBAP, 300 μ M) and manganese (III) tetrakis(1-methyl-4-pyridyl)porphyrin (MnTMPyP, 100 μ M) (16, 17), also reversed PALM-induced IR (Fig. 2E). Since MnTBAP can substitute for the endogenous mitochondrial MnSOD *in vivo* (18) we tested this compound against a range of IR models including CI, TNF, and DEX in both 3T3-L1 adipocytes and L6 myotubes and found that MnTBAP reversed all models of IR (Fig. 2F and G).

These data suggest that mitochondrial O₂^{•-} is a common feature across multiple models of IR. To confirm the findings obtained with these drugs and antioxidants we used a more specific genetic strategy by overexpressing MnSOD. Overexpression of MnSOD by 2.5-fold had no significant effect on insulin-stimulated GLUT4 translocation in control L6 cells but overcame the ability of CI, TNF, DEX, and PALM to impair insulin-stimulated GLUT4 translocation (Fig. 2H). In insulin resistant cells but not in control cells, overexpression of MnSOD led to an overshoot in insulin-stimulated GLUT4 translocation (Fig. 2H). One possibility is that these IR models still induce mitochondrial O₂^{•-}, however its rapid conversion to hydrogen peroxide (H₂O₂) by the overexpressed MnSOD may somehow potentiate insulin action. Such a model has been described for growth factor-induced H₂O₂ production, which inhibits tyrosine phosphatases to enhance signal transduction (19). However, overexpression of MnSOD overcame IR without significantly modulating insulin signaling (Fig. 2I), suggesting that if H₂O₂ is responsible for the overshoot it must be mediating its effects via an alternate mechanism.

Mitochondrial Superoxide Is Sufficient to Drive IR. The above findings show that many models of IR are associated with increased mitochondrial O₂^{•-}, which if reversed may restore insulin sensitivity. We next investigated whether the induction of mitochondrial O₂^{•-} within the ETC under defined experimental conditions is sufficient to drive IR. Complex III (cytochrome *bc*₁) of the ETC is a well established source of mitochondrial O₂^{•-} so we selectively induced O₂^{•-} formation with the Complex III Q_i site inhibitor antimycin A (AntA) (20, 21). Low doses of AntA (50 nM) caused a rapid (30 min) decrease in insulin-stimulated GLUT4 translocation

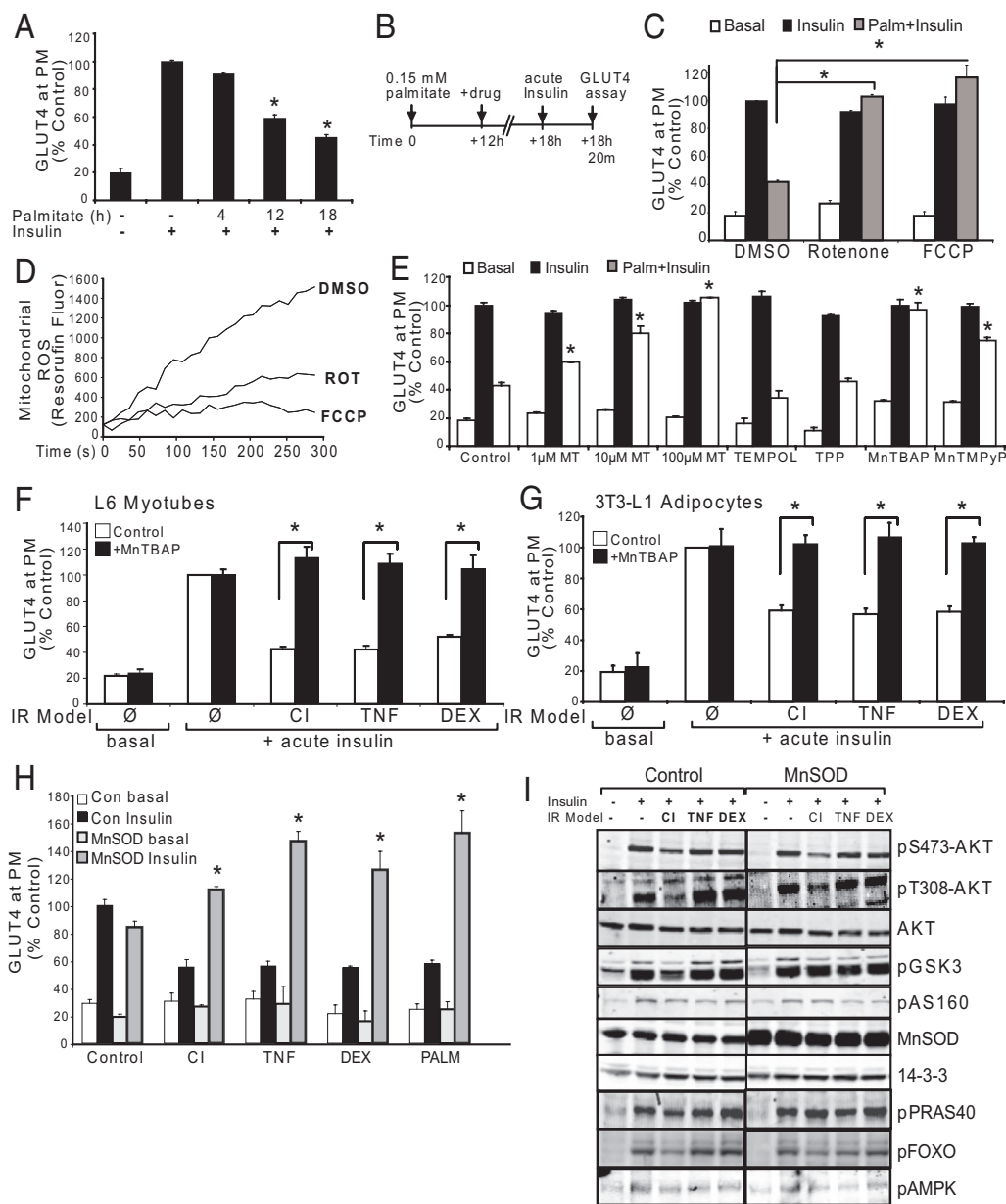


Fig. 2. Inhibition of mitochondrial superoxide production reverses IR in vitro. (A) L6 myotubes were treated with carrier control or 0.15 mM palmitate for 4, 12, or 18 h before acute insulin stimulation and analysis of surface HA-GLUT4. (B) Experimental design. L6 myotubes become insulin resistant within the first 12 h of 0.15 mM PALM treatment (as shown in A). At this time the media was refreshed $-/+$ drug treatment for the final 6 h before acute insulin stimulation and analysis of PM-GLUT4. (C) Myotubes were incubated with 100 nM FCCP, 10 nM rotenone, or control (DMSO) for the final 6 h of 18 h 0.15 mM palmitate incubation as described in (B). (D) Isolated mitochondria from L6 cells were incubated in the presence of DMSO, 100 nM FCCP, or 10 nM Rotenone and Amplex Red oxidation to Resorufin was monitored as an indication of mitochondrial ROS production. Line tracings from a representative experiment are shown. (E) As described in (B), palmitate treated myotubes were incubated with the mitochondrial SOD mimetics MitoTEMPO (MT), 300 μ M MntBAP, 100 μ M MntTMPYP, or controls water, TPP (1 mM), and TEMPOL (1 mM). All antioxidants except TEMPOL (cytoplasmic SOD mimetic) reversed palmitate-induced IR. (F–G) L6 myotubes (F) or 3T3-L1 adipocytes (G) were treated with CI, TNF, or DEX; during the final 6 h the cells were incubated with control (water, open bars) or MntBAP (300 μ M, black bars). (H) L6 myotubes overexpressing MnSOD were protected from PALM, CI, TNF, and DEX-induced IR whereas control cells displayed marked IR under the same conditions as defined by reduced insulin-stimulated surface HA-GLUT4. (I) Representative Western blots of MnSOD over-expressing myotubes and empty vector control myotubes treated with IR models. 14–3–3 is shown as a loading control. (A, C, E–G) Results are displayed as means \pm SEM, $n = 3$.

tion in L6 myotubes (Fig. 3A) concomitant with increased $O_2^{\cdot-}$ production from mitochondria (Fig. 3B). To exclude the possibility that partial inhibition of mitochondrial electron transfer rather than $O_2^{\cdot-}$ production explained the effects of AntA, we performed three further experiments. First, stigmatellin, which blocks AntA-induced $O_2^{\cdot-}$ production by inhibiting the transfer of electrons to the AntA-binding site of complex III (21), was shown to prevent AntA-induced IR (Fig. 3C). Second, the mitochondrial SOD mimetics MntBAP and MitoTEMPO were protective against AntA-induced IR (Fig. 3D), and third, overexpression of MnSOD in L6 cells prevented AntA-induced IR (Fig. 3E). Again, MnSOD overexpression led to supercompensation of insulin-stimulated GLUT4 translocation only in cells treated with an insult (Fig. 3E), similar to the effect seen with other IR models (Fig. 2H). Notably, the inhibitory effect of AntA on insulin-stimulated GLUT4 was not due to inhibition of signal transduction through Akt as evidenced by normal Akt phosphorylation at both maximal (Fig. 3F) and sub-maximal insulin concentrations (Fig. S1) in the presence of AntA.

Mitochondrial Superoxide Production Regulates Insulin Action in Vivo.

The studies described above provide strong evidence for the involvement of mitochondrial $O_2^{\cdot-}$ production in multiple models of IR in muscle and fat cells in vitro. To confirm these findings in a physiological setting we used three approaches. First, we showed that acute administration of MntBAP to high fat fed mice caused a significant improvement in glucose tolerance (Fig. 4A and B) principally due to increased peripheral insulin sensitivity in muscle and fat (Fig. 4C and D). Next, we examined the effects of MnSOD overexpression using transgenic (TG) mice expressing this enzyme under the control of the endogenous mouse promoter. The MnSOD-TG mice displayed a 2- to 2.5-fold increase in MnSOD expression in muscle and fat (Fig. S2A), normal body weight (Fig. S2B), and similar glucose tolerance vs. wild-type (WT) mice fed a standard low fat diet (LFD, Fig. 4E). We then challenged these same mice with a high fat diet (HFD) for one week. WT animals had impaired glucose tolerance under these conditions; however, this was not the case for MnSOD-TG mice (Fig. 4F). Importantly,

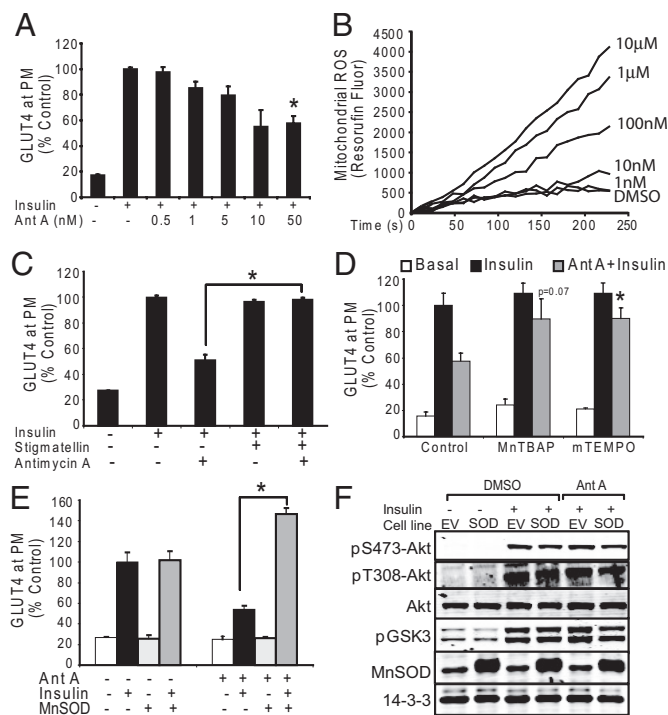


Fig. 3. Mitochondrial superoxide production is sufficient to drive insulin resistance in vitro. (A) Antimycin A treatment for 10 min before acute 100 nM insulin stimulation (20 min) causes IR. (B) Antimycin A induces ROS production from isolated mitochondria at low nM concentrations. Line tracings from a representative experiment of three are shown. (C) L6 myotubes treated with 100 nM stigmatellin for 10 min before 50 nM Antimycin A were protected from IR. (D) L6 myotubes treated with 300 μ M MnTBAP or 100 μ M MitoTEMPO for 20 min before 50 nM Antimycin A were protected from IR. (E) MnSOD over-expressing L6 myotubes were protected from 50 nM Antimycin A induced IR. (F) Antimycin A treatment 10 min before 20 min of acute 100 nM insulin stimulation did not affect insulin-stimulated pS473-Akt, pT308-Akt, pFOXO, pPRAS40, pAMPK, or pGSK3. EV = empty vector, SOD = MnSOD overexpressing cells. (A, C–E) Results are displayed as means \pm SEM, $n = 3$.

there was no change in food intake (Fig. S2C), body weight gain (Fig. S2B), or insulin secretion (Fig. 4G) during the glucose tolerance test. To determine if MnSOD overexpression also protected against the effects of long-term high-fat feeding, we subjected another cohort of mice to a standard LFD or HFD for 12 weeks. Both WT and MnSOD-TG mice accrued the same amount of body mass (Fig. S2D), however, the MnSOD-TG mice were partially protected against HFD-induced glucose intolerance compared to WT animals (Fig. 4H). Accordingly, insulin tolerance tests showed that MnSOD-TG remained more insulin responsive than WT controls when fed a HFD for up to 24 weeks (Fig. 4I). These effects occurred despite no significant change in circulating triglyceride or free fatty acid levels between WT and MnSOD-TG mice fed chow or HFD (Fig. S3). These data confirm our in vitro studies where L6 muscle cells overexpressing MnSOD were also protected from IR.

To examine whether reduced mitochondrial $O_2^{\bullet-}$ scavenging capacity might be sufficient to cause IR in vivo, we tested glucose tolerance in MnSOD deficient mice. Homozygous deletion of MnSOD is lethal, whereas MnSOD^{-/+} mice have no significant change in longevity or body weight regulation and breed normally (22). MnSOD^{-/+} mice displayed a 70% reduction in MnSOD protein in muscle and fat compared to WT littermates (Fig. S1E), that was associated with a significant impairment in glucose tolerance on standard LFD (Fig. 4J) despite similar insulin levels to control mice (Fig. 4K).

Discussion

While a general link between IR and oxidative stress has been proposed (23–25), evidence supporting a specific role for mitochondrial $O_2^{\bullet-}$ in IR in muscle and fat cells is scarce (26). Mitochondrial $O_2^{\bullet-}$ is primarily formed at Complex I (NADH dehydrogenase) or Complex III (cytochrome *bc*₁) of the ETC (11, 14, 21). Since these electron transfer steps are nonenzymatic, any process that increases the reduced state of these electron carriers will increase the probability for electron extraction by high reduction potential molecules, such as molecular oxygen (to create $O_2^{\bullet-}$) (11). Thus, increased mitochondrial oxidative phosphorylation due to increased influx of nutrients in the absence of increased ATP consumption may be expected to increase mitochondrial $O_2^{\bullet-}$ production due to depletion of ADP availability and increased occupancy of electron carriers. Similarly, a reduction in mitochondrial number without a concomitant reduction in nutrient uptake will increase net substrate flux through the remaining mitochondria resulting in increased $O_2^{\bullet-}$ production per energy unit. Additionally, aged mitochondria become damaged and concomitantly produce more mitochondrial ROS per unit mitochondria compared to young mitochondria (27). Thus, mitochondrial $O_2^{\bullet-}$ production may represent the link between mitochondrial function and IR.

Mitochondrial $O_2^{\bullet-}$ has previously been linked to hyperglycemia-induced metabolic dysfunction in endothelial cell systems (28) and in inflammation in adipocytes (29). A major advance of the present study is the observation that mitochondrial $O_2^{\bullet-}$ is upstream of IR in skeletal muscle and adipose tissue. Using a mitochondria-targeted dye that is highly specific for $O_2^{\bullet-}$ we show increased $O_2^{\bullet-}$ production in four separate models of IR, and it has recently been reported that in vitro preparations of muscle mitochondria from mice fed a high diet are more susceptible to ROS production (25). However, in these studies mitochondrial H_2O_2 rather than $O_2^{\bullet-}$ was proposed as the link to IR. In our study we have overexpressed MnSOD in cell lines and in animals and show that this alone has significant insulin sensitizing properties under various cellular and physiologic stresses. This is intriguing since MnSOD selectively decreases $O_2^{\bullet-}$ levels at the expense of increased H_2O_2 production and so this supports a role for $O_2^{\bullet-}$ rather than H_2O_2 in IR. It is also of interest that overexpression of MnSOD in L6 cells had no effect on insulin action in control cells whereas in insult-treated cells we observed a supercompensatory effect on insulin action. This indicates that $O_2^{\bullet-}$ production is increased under these conditions and its rapid dismutation to H_2O_2 may be mediating a positive effect on insulin action (26). It should be noted that longer term exposure of cells to high levels of H_2O_2 leads to IR (26). However, this occurs via covalent modification of Akt, an effect that we have not observed in more physiological models of IR (5).

There are several features of $O_2^{\bullet-}$ that make it an ideal sensor of cellular nutrient homeostasis, which are not shared by H_2O_2 . Unlike H_2O_2 , $O_2^{\bullet-}$ is membrane impermeable and so its production will be relatively localized and concentrated allowing for reliable detection and restricting its cadre of substrates. Additionally, the chemical spin state of $O_2^{\bullet-}$ makes it relatively target specific such that its known substrates include a brief list of other radicals such as nitric oxide, Fe/S containing proteins, and phosphatases such as PTP1B and PP2B (30). Finally, $O_2^{\bullet-}$ is proximal to H_2O_2 thus it likely represents a very early sign of cellular stress. $O_2^{\bullet-}$ may act as a conduit to induce a range of cellular preservation pathways directed toward minimizing further $O_2^{\bullet-}$ production. Other known roles for $O_2^{\bullet-}$ include increasing mitochondrial uncoupling and increased expression of antioxidant genes. Based upon the present study, $O_2^{\bullet-}$ also leads to IR, which may represent a third key component of this antioxidant defense mechanism. This hypothesis is exciting for a number of reasons. For example, it suggests that IR may be a protective mechanism, in which case we

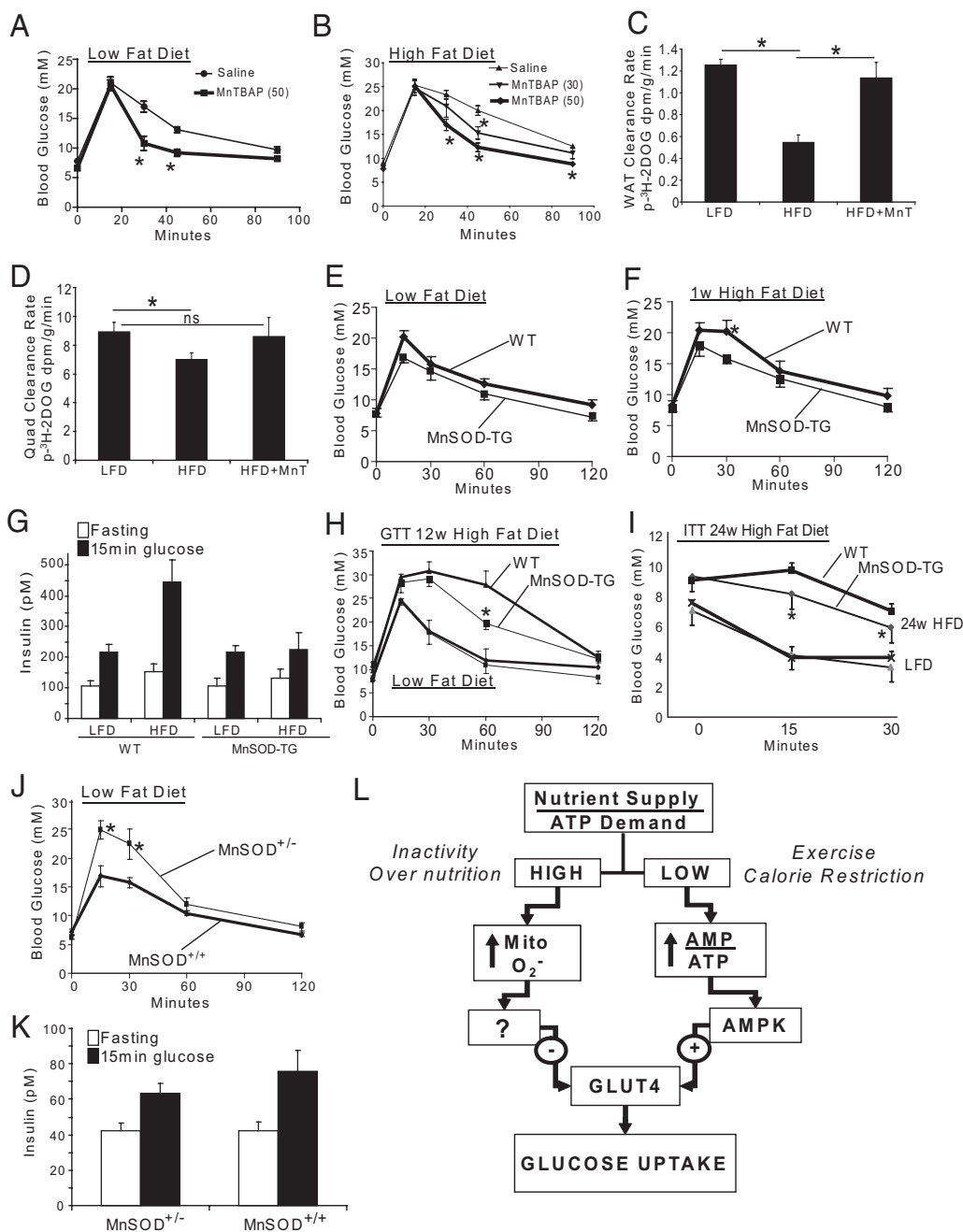


Fig. 4. Mitochondrial superoxide regulates insulin sensitivity in vivo. (A and B) Mice fed a standard low fat (LFD, A) or high fat diet (HFD, B) \pm 30 or 50 mg/kg MnTBAP 6 h before i.p. injection of 1.5 g glucose/kg body weight. $n \geq 8$ mice per group. (C and D) Glucose disposal into muscle and gonadal adipose tissue was measured by GTT with $^3\text{H-2DOG}$ tracer. Mice were fed LFD or 2 weeks HFD \pm 50 mg/kg MnTBAP (HFD+MnT) 6 h before glucose tolerance testing. $n = 5$ mice per group. (E and F) GTTs (1.5 g glucose/kg body weight) were performed on MnSOD transgenic (MnSOD-TG) and age matched control (WT) mice fed a LFD then switched to HFD for 1 week. The same mice were used in both tests, $n = 7\text{--}8$ mice. (G) For the experiment in E-F above, insulin levels were measured after 6 h fasting and 15 min after glucose injection. $n = 7$. (H) GTT of MnSOD-TG and age matched WT mice fed a LFD or HFD for 12 weeks. $n = 3\text{--}4$ for LFD and 5–6 for HFD. (I) Insulin tolerance test (ITT) of MnSOD-TG and age matched WT mice fed a LFD or HFD for 24 weeks. $n = 7\text{--}8$ in each group. (J) GTT of MnSOD heterozygous (MnSOD^{+/-}) vs. WT mice fed a LFD. $n = 6\text{--}8$ mice. (K) Insulin levels were measured after the 6 h fast and 15 min after glucose injection in (J). $n = 6\text{--}8$. (L) Proposed model for the intrinsic control of glucose entry into muscle and fat cells. The ratio between nutrient supply and ATP demand is at the center of this mechanism such that when this ratio is imbalanced a rapid compensatory cellular response can acutely correct energy shortage or surplus by controlling glucose entry into the cell. It is well-accepted that when cellular nutrient supply/ATP demand is low (e.g., exercise or calorie restriction) the concomitant increase in the AMP/ATP ratio leads to activation of AMPK and subsequently the increase in glucose uptake independent of insulin. However, in the opposite situation, when nutrient supply/ATP demand is high (e.g., nutrient oversupply or inactivity) we propose that the ensuing increase in mitochondrial superoxide production is the signal that drives a cellular response to dampen glucose uptake via the antagonism of GLUT4.

should perhaps reconsider using therapeutic strategies to overcome unless they also eliminate the primary defect. Moreover, it suggests that cells have evolved sophisticated mechanisms to not only guard against nutrient lack, such as the AMPK pathway, but also nutrient excess (Fig. 4L). For most organisms the latter is presumably quite rare or at least an intermittent phenomenon emphasizing why the current situation of constant nutrient oversupply is not easily tolerated.

Two significant questions arise from this study. First, how does $\text{O}_2^{\cdot-}$ produced in the mitochondria regulate the translocation of GLUT4 to the plasma membrane? Intriguingly, cells that lack mitochondria are not insulin responsive (31), suggesting that the insulin signal must traverse this organelle as a checkpoint before signaling to GLUT4. Second, is mitochondrial antioxidant therapy

likely to be of benefit in the treatment of metabolic disease? One potential problem is that while this strategy may alleviate oxidative damage it may impair hormetic feedback pathways or lead to alternate problems of cellular over nutrition including advanced glycation end products, which are also linked to IR. Thus, care must be taken when considering this type of intervention.

In summary, the fact that mitochondrial $\text{O}_2^{\cdot-}$ is upstream of IR is of major significance suggesting that IR may be part of the antioxidant defense mechanism to protect cells from further oxidative damage. Thus, IR may be viewed as an appropriate response to increased nutrient accumulation as originally suggested by Unger (32), representing part of the cells attempt to return to an energy neutral situation. This concept potentially changes our thinking concerning therapeutic modes of treating metabolic disease.

Methods

Cell Culture Models of IR. 3T3-L1 adipocytes and L6 myotubes overexpressing HA-GLUT4 were used for all in vitro experiments. HA-GLUT4 is essential for the measurement of GLUT4 at the plasma membrane (PM) as described in ref. 5. Models of IR were performed as described here. Chronic insulin (CI) treated cells were cultured in serum free DMEM media with 0.2% BSA (stepdown media) and given doses of 10 nM insulin at 12 PM, 4 PM, 8 PM, and 8 AM the following day. At 12 PM the cells were washed three times with PBS and incubated in stepdown media for 90 min before experimentation. Palmitate (PALM) treatment was performed essentially as described in ref. 5, with the exception that the cells were serum free for the entire 18 h of treatment. Dexamethasone (DEX) treatment consisted of 24 h incubation with 1 μ M dexamethasone in stepdown media before experimentation. Finally, inflammation was mimicked with 2 ng/mL tumor necrosis factor α (TNF). TNF was added at 1:30 PM each day for 4 days with the final day in SF media. In experiments where drugs were added to the IR models the compounds remained on the cells with the insults for the entire duration of the final 6 h, except in the case of CI where the drugs were washed out during the PBS washes but replaced for the final 90 min. MnSOD cDNA was obtained from JA Melendez (Albany Medical College, NY) and cloned into the retroviral vector pBABE-puro. MnSOD and empty vector control retroviruses were produced in Platinum-E cells and used to infect L6 myoblasts overexpressing HA-GLUT4 driven from a pWZL-derived retrovirus. Cells were stably selected with G418 (400 μ g/mL) and puromycin (2 μ g/mL) for >3 passages before differentiation and experimentation. TNF and DEX treatment increased cellular GLUT4 levels by 22 and 94%, as described in ref. 5, however in all experiments cell surface GLUT4 was normalized to total cellular GLUT4 thus taking into account changes in GLUT4 expression.

Measurement of Mitochondrial ROS. MitoSOX Red was administered essentially as described by the manufacturer (Molecular Probes); however, the two cell lines required different concentrations and incubation times. L6 myotubes were incubated with 5 μ M MitoSOX Red for the final hour of IR treatment while 3T3-L1 adipocytes were incubated with 1 μ M MitoSOX Red for the final 30 min of treatment. Cells were cultured in low-absorbance, black-walled 96-well plates. After MitoSOX treatment cells were quickly washed with PBS and fluorescence was detected on a Fluo-Star plate reader with excitation at 390 or 485 nm and emission settings at 590 nm.

ROS production by isolated mitochondria was measured by monitoring Amplex Red oxidation to Resorufin in the presence of HRP (ex/em at 540/590 nm). Mitochondria were isolated from L6 cells using a cell culture mitochondrial

isolation kit (Pierce). Isolated mitochondria were resuspended in KCl buffer (125 mM KCl, 20 mM HEPES, 2 mM MgCl₂, 2 mM KH₂PO₄, and 40 μ M EGTA, pH 7.2) containing 1 mM pyruvate and 7 mM succinate and diluted to 0.5 mg/mL. ROS production was measured by adding 50 μ M Amplex Red and 0.1 U/mL HRP and monitoring Resorufin fluorescence over time.

Materials. Antibodies against p-Akt and p-GSK3 were from Cell Signaling. pT642-AS160 antibody was from Symanis. MitoSOX Red was from Invitrogen. MitoTEMPO, MnTBAP, and MnTMPyP were purchased from Alexis Biochemicals. Rotenone, Stigmatellin, AntA, FCCP, and TEMPOL were purchased from Sigma. MnTBAP was prepared in haemacel for use in mice and water for use in cell culture.

Animals. MnTBAP experiments were performed in male C57BL/6 mice at the Garvan Institute and experiments in MnSOD-TG and MnSOD^{-/-} mice were performed at the University of Texas Health Science Center at San Antonio (UTHSCSA). Food and water were provided ad libitum until the date of study and all animal care was in compliance with the US National Institutes of Health and the Australian National Health and Medical Research Council guidelines, as well as institutional guidelines at both Garvan and UTHSCSA. i.p. glucose tolerance tests were performed after a 6 h fast (8 AM–2 PM) and insulin was measured using an ultrasensitive mouse insulin ELISA from Crystal Chem. The HFD used at the Garvan (45% kcal from fat) was made in house as described in ref. 33 and the Garvan LFD (8% calories from fat) was from Gordon's Specialty Stock Feeds. The MnSOD-Tg mice and WT controls were fed HFD (45% kcal from fat, 58V8) or LFD (10% kcal from fat, 58Y2) from Purina Test diets. The MnSOD^{-/-} and WT controls were fed Harlan Teklad 7912.

Statistical Analyses. Data are expressed as means \pm standard error. For GLUT4 translocation analysis each experiment was normalized to maximal insulin stimulation of control cells and this value was set to 100%. *P* values were calculated by two-tailed Student's *t* test using Microsoft excel (Microsoft Corp) or Graph Pad Prism. Statistical significance was set at *P* < 0.05.

ACKNOWLEDGMENTS. This work was supported by the National Institutes of Health Grants DK067509 (to D.E.J.), F32 DK075249 (to K.L.H.), R378G26557 (to A.R. and H.V.R.), and T32 AG021890 (to A.B.S.) and the Diabetes Australia Research Trust and Viertel Foundation Trust (to K.L.H.). N.T. is supported by a Career Development Award and G.J.C., E.W.K., and D.E.J. by Research Fellowships from the National Health and Medical Research Council of Australia. A.R., H.V.R., and H.B.S. are supported by the San Antonio Nathan Shock Center for Excellence in the Basic Biology of Aging. A.J.H. is supported by a University of New South Wales Australian Postgraduate Award.

- Gerstein HC, et al. (2008) Effects of intensive glucose lowering in type 2 diabetes. *N Engl J Med* 358:2545–2559.
- Savage DB, Petersen KF, Shulman GI (2007) Disordered lipid metabolism and the pathogenesis of insulin resistance. *Physiol Rev* 87:507–520.
- Holland WL, et al. (2007) Inhibition of ceramide synthesis ameliorates glucocorticoid-, saturated-fat-, and obesity-induced insulin resistance. *Cell Metab* 5:167–179.
- Taniguchi CM, Emanuelli B, Kahn CR (2006) Critical nodes in signalling pathways: Insights into insulin action. *Nat Rev Mol Cell Biol* 7:85–96.
- Hoehn KL, et al. (2008) IRS1-independent defects define major nodes of insulin resistance. *Cell Metab* 7:421–433.
- Frojdo S, Vidal H, Pirola L (2009) Alterations of insulin signaling in type 2 diabetes: A review of the current evidence from humans. *Biochim Biophys Acta* 1792:83–92.
- Roussel D, Dumas JF, Simard G, Malthiery Y, Ritz P (2004) Kinetics and control of oxidative phosphorylation in rat liver mitochondria after dexamethasone treatment. *Biochem J* 382:491–499.
- Samavati L, Lee I, Mathes I, Lottspeich F, Huttemann M (2008) Tumor necrosis factor α inhibits oxidative phosphorylation through tyrosine phosphorylation at subunit I of cytochrome *c* oxidase. *J Biol Chem* 283:21134–21144.
- Hall JC, Sordahl LA, Stefko PL (1960) The effect of insulin on oxidative phosphorylation in normal and diabetic mitochondria. *J Biol Chem* 235:1536–1539.
- Ross MF, et al. (2005) Lipophilic triphenylphosphonium cations as tools in mitochondrial bioenergetics and free radical biology. *Biochemistry (Mosc)* 70:222–230.
- Turrens JF (1997) Superoxide production by the mitochondrial respiratory chain. *Biosci Rep* 17:3–8.
- Amara CE, et al. (2007) Mild mitochondrial uncoupling impacts cellular aging in human muscles in vivo. *Proc Natl Acad Sci USA* 104:1057–1062.
- Nishikawa T, et al. (2000) Normalizing mitochondrial superoxide production blocks three pathways of hyperglycaemic damage. *Nature* 404:787–790.
- Boveris A, Chance B (1973) The mitochondrial generation of hydrogen peroxide. General properties and effect of hyperbaric oxygen. *Biochem J* 134:707–716.
- Becker LB, vanden Hoek TL, Shao ZH, Li CQ, Schumacker PT (1999) Generation of superoxide in cardiomyocytes during ischemia before reperfusion. *Am J Physiol* 277:2240–2246.
- Korge P, Weiss JN (2006) Redox regulation of endogenous substrate oxidation by cardiac mitochondria. *Am J Physiol Heart Circ Physiol* 291:1436–1445.
- Li QY, Pedersen C, Day BJ, Patel M (2001) Dependence of excitotoxic neurodegeneration on mitochondrial aconitase inactivation. *J Neurochem* 78:746–755.
- Melov S, et al. (1998) A novel neurological phenotype in mice lacking mitochondrial manganese superoxide dismutase. *Nat Genet* 18:159–163.
- Aslan M, Ozben T (2003) Oxidants in receptor tyrosine kinase signal transduction pathways. *Antioxid Redox Signal* 5:781–788.
- Ksenzenko M, Konstantinov AA, Khomutov GB, Tikhonov AN, Ruuge EK (1983) Effect of electron transfer inhibitors on superoxide generation in the cytochrome bc1 site of the mitochondrial respiratory chain. *FEBS Lett* 155:19–24.
- Raha S, McEachern GE, Myint AT, Robinson BH (2000) Superoxides from mitochondrial complex III: The role of manganese superoxide dismutase. *Free Radic Biol Med* 29:170–180.
- Van Remmen H, et al. (2003) Life-long reduction in MnSOD activity results in increased DNA damage and higher incidence of cancer but does not accelerate aging. *Physiol Genomics* 16:29–37.
- Houstis N, Rosen ED, Lander ES (2006) Reactive oxygen species have a causal role in multiple forms of insulin resistance. *Nature* 440:944–948.
- Bonnard C, et al. (2008) Mitochondrial dysfunction results from oxidative stress in the skeletal muscle of diet-induced insulin-resistant mice. *J Clin Invest* 118:789–800.
- Anderson EJ, et al. (2009) Mitochondrial H₂O₂ emission and cellular redox state link excess fat intake to insulin resistance in both rodents and humans. *J Clin Invest* 119:573–581.
- Bashan N, Kovsan J, Kachko I, Ovadia H, Rudich A (2009) Positive and negative regulation of insulin signaling by reactive oxygen and nitrogen species. *Physiol Rev* 89:27–71.
- Savitha S, Panneerselvam C (2006) Mitochondrial membrane damage during aging process in rat heart: Potential efficacy of L-carnitine and DL alpha lipoic acid. *Mech Ageing Dev* 127:349–355.
- Brownlee M (2001) Biochemistry and molecular cell biology of diabetic complications. *Nature* 414:813–820.
- Lin Y, et al. (2005) The hyperglycemia-induced inflammatory response in adipocytes: The role of reactive oxygen species. *J Biol Chem* 280:4617–4626.
- Namgaladze D, Shcherbyna I, Kienhofer J, Hofer HW, Ullrich V (2005) Superoxide targets calcineurin signaling in vascular endothelium. *Biochem Biophys Res Commun* 334:1061–1067.
- Park SY, et al. (2005) Depletion of mitochondrial DNA causes impaired glucose utilization and insulin resistance in L6 GLUT4myc myocytes. *J Biol Chem* 280:9855–9864.
- Unger RH (2003) Lipid overload and overflow: Metabolic trauma and the metabolic syndrome. *Trends Endocrinol Metab* 14:398–403.
- Turner N, et al. (2007) Excess lipid availability increases mitochondrial fatty acid oxidative capacity in muscle: Evidence against a role for reduced fatty acid oxidation in lipid-induced insulin resistance in rodents. *Diabetes* 56:2085–2092.